M.L.G.). The instrumentation is supported by a NSF Regional Instrumentation Facility Grant to the University of Nebraska (CHE 8211164).

Registry No. 1, 90823-18-0; **2**, 90823-19-1; **3**, 90823-20-4; **4**, 90823-21-5; **5**, 90823-22-6; **6**, 90823-23-7; **7**, 90823-24-8; **8**, 90823-25-9; **9**, 90823-26-0; **10**, 90823-27-1; **12**, 90823-28-2; Fe(1-heptene)$^+$, 90823-29-3; Fe(1-nonene)$^+$, 90823-30-6; Fe(1-decene)$^+$, 90823-31-7; Fe(1-dodecene)$^+$, 90823-32-8; Fe(1-tetradecene)$^+$, 90823-33-9; $Fe(CO)_5$, 13463-40-6; $Fe(CO)_2^+$, 35038-15-4; $Fe(CO)^+$, 35038-14-3; Fe^+, 14067-02-8; 1-hexene, 592-41-6; 1-heptene, 592-76-7; 1-octene, 111-66-0; *trans*-2-octene, 13389-42-9; cyclobutane, 287-23-0; methylcyclopropane, 594-11-6; $(ethylene)_2$, 16482-32-9; 1-butene, 106-98-9; *cis*-2-hexene, 7688-21-3; *cis*-3-hexene, 7642-09-3; *cis*-3-methyl-2-pentene, 922-62-3; 1-heptene, 592-76-7; 2-methyl-1-heptene, 15870-10-7; isobutene, 115-11-7; 2-methyl-1-pentene, 763-29-1; 2-methyl-2-pentene, 625-27-4; cyclopropane, 75-19-4; propene, 115-07-1; 1-pentene, 109-67-1; 2-methyl-1-butene, 563-46-2; 3-methyl-1-butene, 563-45-1; 2-methyl-2-butene, 513-35-9; *trans*-2-pentene, 646-04-8; *cis*-2-pentene, 627-20-3; *trans*-3-octene, 14919-01-8; *cis*-3-octene, 14850-22-7; 2-methyl-2-heptene, 627-97-4; cyclopentane, 287-92-3; bis(propene), 16813-72-2; 1-nonene, 124-11-8; *trans*-2-hexene, 4050-45-7; *trans*-4-octene, 14850-23-8; *cis*-4-octene, 7642-15-1; *trans*-3-hexene, 13269-52-8; 4-methyl-3-heptene, 4485-16-9; 3-methyl-3-heptene, 7300-03-0; 3-methyl-2-pentene, 922-61-2; cyclohexane, 110-82-7; 1,3-pentadiene, 504-60-9; 1,4-pentadiene, 591-93-5; isoprene, 78-79-5; 2-methyl-2-pentene, 922-61-2; cyclohexane, 110-83-8; 1,5-hexadiene, 592-42-7; benzene, 71-43-2; 1,3,5,7-cyclooctatetraene, 629-20-9; $Fe(CO)_3$-cyclohexadiene, 12152-72-6; 1,5-hexadiyne, 628-16-0; *cis*-2-octene, 7642-04-8; *cis*-3-methyl-3-heptene, 22768-18-9.

Determination of the Aluminum-27 Spin–Lattice Relaxation Rate and the Relative Number of Each Chloroaluminate Species in the Molten 1-*n*-Butylpyridinium Chloride/$AlCl_3$ System

T. Matsumoto and K. Ichikawa*

Contribution from the Department of Chemistry, Faculty of Science, Hokkaido University, Sapporo 060, Japan. *Received June 9, 1983*

Abstract: ^{27}Al longitudinal magnetization recovery curves were measured by using the inversion recovery method on molten 1-*n*-butylpyridinium chloride/$AlCl_3$ mixtures at various components of 39–80 mol % $AlCl_3$ and between 30 °C and 75 °C. The recovery curves did not show single exponential decays at the components located between the two stoichiometries (e.g., between 50 and 67 mol % $AlCl_3$), in contrast with the single exponential decays observed in melts at less than 50 mol % $AlCl_3$ and at 67 mol % $AlCl_3$. The composition dependence of the individual relaxation rates $R_{1,\alpha}$ and the individual concentrations X_α of each main chloroaluminate species, α, such as $AlCl_4^-$, $Al_2Cl_7^-$, $Al_3Cl_{10}^-$, or Al_2Cl_6, were obtained by fitting a model associated with the chemical exchange process from species A to B into the observed nonlinear logarithmic recovery curve. The remarkably slow exchange rate (i.e., the long exchange lifetime) was comparable with the relaxation rates in magnitude, and it gave rise to the nonlinear nature in the logarithmic recovery curves. The chemical exchange from species A to B promotes the individual relaxation of ^{27}Al in each species α. This is because the relaxation rate is the minimum in magnitude for the melt at the BPCl-rich side of 50 mol % $AlCl_3$ or at the stoichiometric composition, in which the chemical exchange from species A to B does not take place. Over all the compositions, the empirical rule among each $R_{1,\alpha}$ is as follows: $R_{1,AlCl_4^-} < R_{1,Al_2Cl_7^-}$, $R_{1,Al_2Cl_7^-} < R_{1,Al_3Cl_{10}^-}$, and $R_{1,Al_2Cl_6} < R_{1,Al_3Cl_{10}^-}$. Here the NMR relaxation of the ^{27}Al nucleus in the melts originates mainly from the interaction between the quadrupolar moment and the electric field gradient fixed at a central Al nucleus by sharing electrons with the chlorines of the nearest neighbors in each species. The dependence of the mole fractions $X(AlCl_4^-)$ and $X(Al_2Cl_7^-)$ of the $AlCl_4^-$ and $Al_2Cl_7^-$ species on the formal composition was consistent with the potentiometric and Raman spectra investigations. Above 67 mol % $AlCl_3$, the other $Al_3Cl_{10}^-$ and Al_2Cl_6 species are present as the main species: a probable peak in the $X(Al_3Cl_{10}^-)$ values locates near the stoichiometry $BPAl_3Cl_{10}$ (or 75 mol % $AlCl_3$), and above 75 mol % $AlCl_3$, the Al_2Cl_6 species becomes a main species upon successive additions of the $AlCl_3$ component.

Considerable interest has been shown recently in chloroaluminate melts such as $AlCl_3$/MCl (M = Li, Na, etc.) and $AlCl_3$/alkylpyridinium halide because of their special properties as acid–base solvents.[1] Raman spectroscopic studies have shown that $AlCl_4^-$, $Al_2Cl_7^-$, $Al_nCl_{3n+1}^-$ ($n \geq 3$), and Al_2Cl_6 are present in their melts.[2,3] The anionic species equilibrium for the dissociation reaction

$$2AlCl_4^- \rightleftarrows Al_2Cl_7^- + Cl^-$$

has been investigated by potentiometry.[4,5] ^{27}Al nuclear magnetic resonance studies on chloroaluminate melts have examined the characteristics of these melts, which consist of the $AlCl_4^-$ and $Al_2Cl_7^-$ ions.[6] To our knowledge, the relaxation phenomena on the ^{27}Al longitudinal and transverse magnetizations have not been investigated, though the ^7Li and ^{23}Na spin–lattice relaxation rates have been obtained in molten $LiAlCl_4$ and $NaAlCl_4$, respectively.[7]

This paper describes an examination of the formal composition dependence of the individual relaxation rates, $R_{1,\alpha}$, and of the mole fractions, X_α, of the main species such as $AlCl_4^-$, $Al_2Cl_7^-$, Al_2Cl_6 and a high polymer assigned tentatively to $Al_3Cl_{10}^-$ by measuring the ^{27}Al longitudinal magnetization recovery curves for the room-temperature melt of 1-*n*-butylpyridinium chloride (BPCl) + $AlCl_3$ mixtures and by reproducing the experimental recovery

(1) Boston, C. R. "Advances in Molten Salt Chemistry"; Braunstein, J., Mamantov, G., Smith, G. P., Eds.: Plenum Press: New York, 1971; Vol. 1, p 219. Jones, H. L.; Osteryoung, R. A. "Advances in Molten Salt Chemistry": Plenum Press: New York, 1975; Vol. 3, p 121. Chum, H. L.; Osteryoung, R. A. "Ionic Liquid"; Inman, D., Lovering, D. G., Eds.; Plenum Press: New York, 1981: p 407.
(2) Gale, R. J.; Gilbert, B.; Osteryoung, R. A. *Inorg. Chem.* **1978**, *17*, 2728.
(3) Rytter, E.; Øye, H. A.; Cyvin, S. J.; Cyvin, B. N.; Klaeiboe, P. J. *Inorg. Nucl. Chem.* **1973**, *35*, 1185.
(4) Gale, R. J.; Osteryoung, R. A. *Inorg. Chem.* **1979**, *18*, 1603.
(5) Torsi, G.; Mamantov, G. *Inorg. Chem.* **1971**, *11*, 1439.
(6) Gray, J. L.; Maciel, G. E. *J. Am. Chem. Soc.* **1981**, *103*, 7147.
(7) Matsumoto, T.; Ichikawa, K. *Bull. Chem. Soc. Jpn.* **1982**, 1100.

0002-7863/84/1506-4316$01.50/0

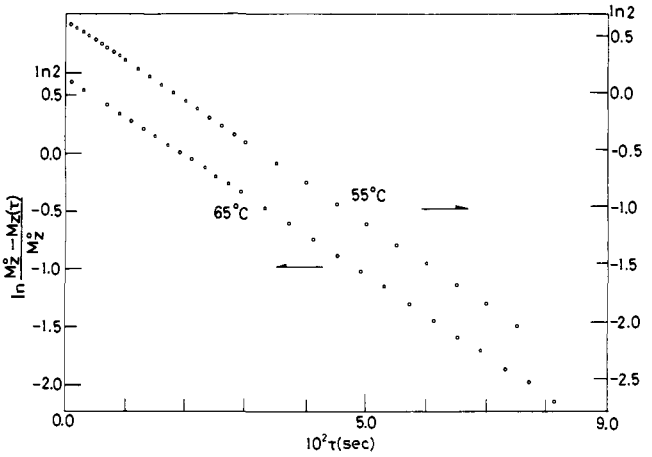

Figure 1. Longitudinal magnetization recovery curves at 45 mol % $AlCl_3$. The main species is denoted as $AlCl_4^-$, and the melts at less than 50 mol % $AlCl_3$ are characteristic of the basic solutions.

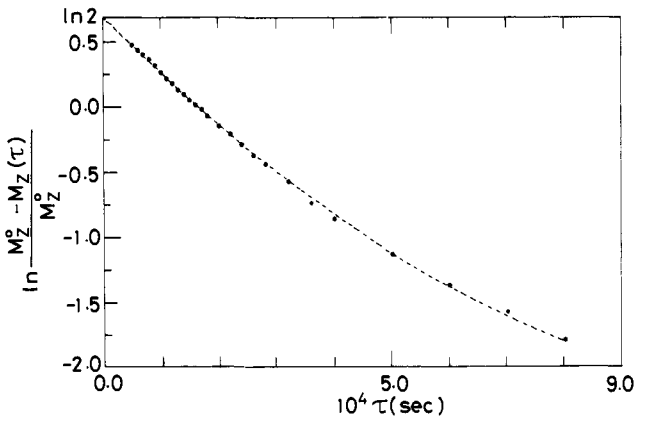

Figure 2. Nonlinear logarithmic recovery curve at 62 ± 2 mol % $AlCl_3$ and 35 °C. The melt consists of the major $AlCl_4^-$ and $Al_2Cl_7^-$ species. The dashed line is a fit using the nonlinear least-square method.

curves using the model associated with the chemical exchange of ^{27}Al under the equilibrium condition among the main chloroaluminate species and Cl^-.

Experimental Section

Materials. BPCl was prepared by the method outlined by Gale, Gilbert, and Osteryoung.[2] The sample of aluminum trichloride used was crystalline. The manipulations of all materials were performed under an argon gas atmosphere in a drybox. The samples were sealed under vacuum into approximately 0.5-cm^2 cross-sectional Pyrex cells for the NMR measurements. The compositions were determined by atomic or electronc absorption spectrochemical analyses for aluminum, by precipitation titration analyses for chlorine, and by the thermal conductivity method for carbon.

NMR Measurements. The NMR measurements were carried out at various compositions of 39–80 mol % $AlCl_3$ between 30 °C and 75 °C. The longitudinal magnetization recovery curves were obtained by using the inversion recovery (or 180°, τ, 90°) method. The instrument used was a Bruker CXP-100; the resonance frequency of aluminum-27 was ca. 23.44 MHz.

Results

The typical logarithmic recovery curves are shown in Figures 1–5 for 45, 62 ± 2, 67, 72 ± 1, and 79 mol % $AlCl_3$, respectively. The inversion recovery method leads to the observed magnetization M_z at τ as follows:

$$M_z(\tau) = M^\circ_z(1 - 2e^{-\tau/T_1}) \quad (1)$$

where $M_z(\tau)$ was measured for ca. 30 values of τ. Figure 6 illustrates the dependence of the spin–lattice relaxation rates R_1 ($\equiv T_1^{-1}$) on the temperature at 45 and 67 mol % $AlCl_3$, where the R_1 values were obtained from the single exponential decays in the logarithmic recovery curve vs. τ (see Figures 1 and 3). The relaxation rate R_1 of the species $AlCl_4^-$ is about 55 ± 5 s^{-1} at 35 °C for melts at less than 50 mol % $AlCl_3$; this is because the dominant aluminum species in the basic melts is $AlCl_4^-$. The recovery curve also shows a single exponential decay at 67 mol % $AlCl_3$, which corresponds to the stoichiometry $BPAl_2Cl_7$, as shown in Figure 3. Since the $Al_2Cl_7^-$ species exists in the melt as a main chloroaluminate species, as far as the available NMR sensitivity permitted us to observe, its R_1 value is equal to ca. 1000 s^{-1} at 35 °C.

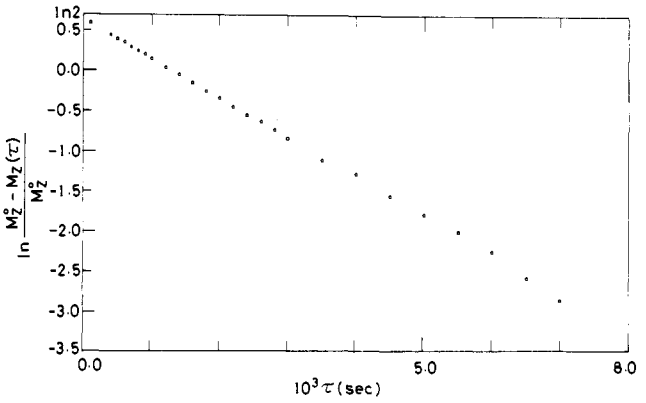

Figure 3. Longitudinal magnetization recovery curve shows the single exponential decay at 67 mol % $AlCl_3$ (i.e., at the stoichiometry $BPAl_2Cl_7$: there exists the $Al_2Cl_7^-$ species as a main species) and at 65 °C.

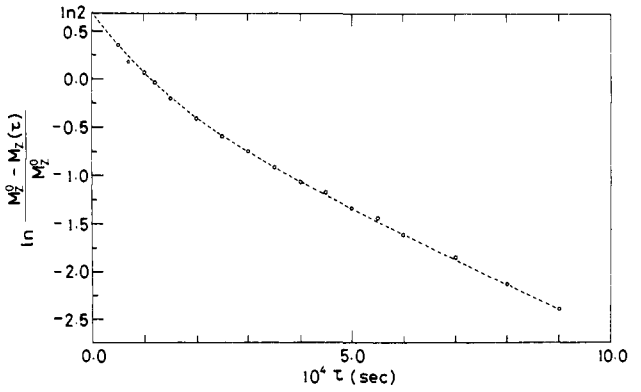

Figure 4. Nonlinear logarithmic recovery curve at 72 ± 1 mol % $AlCl_3$ and 35 °C, at which the melt consists of the major $Al_3Cl_{10}^-$ and $Al_2Cl_7^-$ species. The dashed line is a fit using the nonlinear least-square method.

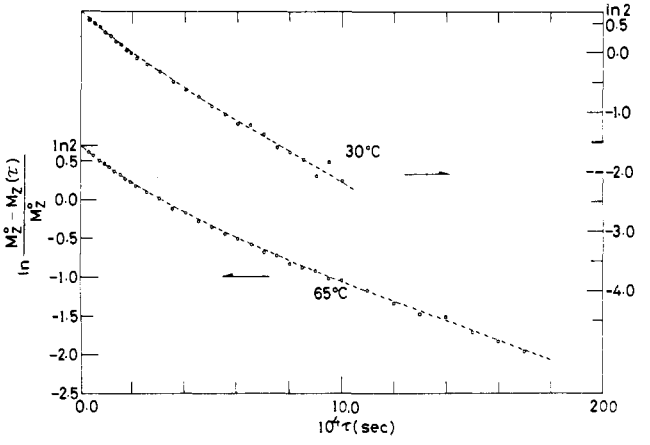

Figure 5. Nonlinear logarithmic recovery curves at 79 mol % $AlCl_3$. The melt consists of the major $Al_3Cl_{10}^-$ and Al_2Cl_6 species. Each dashed line is a fit using the nonlinear least-square method.

On the other hand, the recovery curves do not show single exponential decays for the many samples having their formal composition located between the two stoichiometric compositions, i.e., (i) at 62 ± 2 mol % $AlCl_3$ between 50 mol % $AlCl_3$ (or at the stoichiometry $BPAlCl_4$) and 67 mol % $AlCl_3$ (or at the stoichiometry $BPAl_2Cl_7$) (see Figure 2), (ii) at 72 ± 1 mol % $AlCl_3$

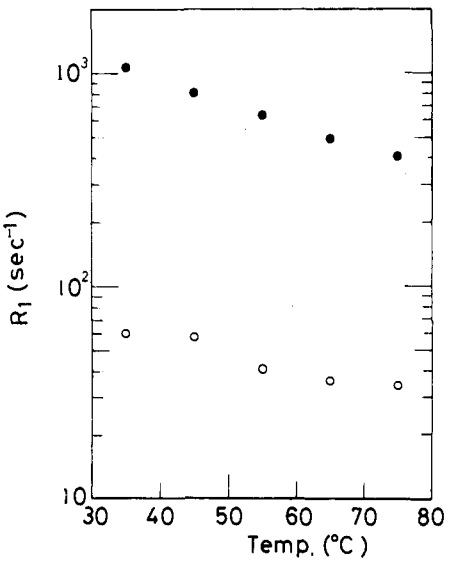

Figure 6. Temperature dependences of the spin–lattice relaxation rates at 45 mol % $AlCl_3$ (○) and 67 mol % $AlCl_3$ (●). They are obtained from the single exponential decays of the longitudinal recovery curves as shown in Figures 1 and 3.

(see Figure 4) between 67 and 75 mol % $AlCl_3$ (or at the stoichiometry $BPAl_3Cl_{10}$), and (iii) at 79 mol % $AlCl_3$ (see Figure 5) between 75 and 100 mol % $AlCl_3$. The observed free induction decay (FID) consists of two signals, which result from the different magnetization components for each main species, because each relaxes to the equilibrium state at different rates. The non-single-exponential recovery curve obtained by means of the accumulation of FID at the time interval t_d between the last 90° pulse and the onset of data acquisition does not give any individual spin–lattice relaxation rates for each chloroaluminate species.[8]

Discussion

The relaxation rate of ^{27}Al in each chloroaluminate species is determined by the NMR relaxation mechanism for spin transition in each species and the probability of chemical exchange from one species to another.

The NMR relaxation mechanism for an aluminum-27 nucleus (spin $I = {}^5/_2$) is expressed in terms of the local electric field gradients (efg), which show that the time dependence is caused mainly by the reorientational motion of each chloroaluminate species in the BPCl + $AlCl_3$ melt. The local efg. established at ^{27}Al nucleus originates chiefly from the electrostatic potential arising from all of the charges in each chloroaluminate species as well as from the unlike and like ions around the species of interest.[9] On the way to the relaxation process, the chemical exchange takes place under the equilibrium condition among the Cl^- ion and chloroaluminate species such as $AlCl_4^-$, $Al_2Cl_7^-$, $Al_3Cl_{10}^-$, and Al_2Cl_6 in the molten BPCl + $AlCl_3$ mixtures. The probability for spin transfer from one species to another promotes the NMR relaxation. The nonlinear nature of the recovery curve (see Figures 2, 4, and 5) results from the sum of the magnetizations, which undertake the time evolution, for the individual chloroaluminate species.

On the basis of the vibrational spectral results of the molten BPCl + $AlCl_3$ mixtures for the 50–66.7 mol % $AlCl_3$, the main chloroaluminate species were assigned to the $AlCl_4^-$ and $Al_2Cl_7^-$ ions.[2] In the basic melts up to 50 mol % $AlCl_3$, an equilibrium constant for the dissociation

$$2AlCl_4^- = Al_2Cl_7^- + Cl^- \quad (2)$$

was determined to be of the order of 10^{-13};[4] there were no Raman vibrational frequencies due to $Al_2Cl_7^-$ present in the spectra of these metals. In the $2AlCl_3$·BPCl melt (or the $BPAl_2Cl_7$ melt), the $AlCl_4^-$ ion is converted virtually completely to the $Al_2Cl_7^-$ ion.[2] In the melts from 50 mol % $AlCl_3$ to 67 mol % $AlCl_3$, aluminum undergoes a chemical exchange from the $AlCl_4^-$ ion to the $Al_2Cl_7^-$ ion. The relaxation process of ^{27}Al in $AlCl_4^-$ changes itself into the relaxation process in the $Al_2Cl_7^-$ ion by the chemical exchange, and vice versa. In the melts which consist of the main A and B species, the relation between each number density of ^{27}Al (N°_A and N°_B) and each chemical exchange lifetime (τ_A and τ_B) is expressed as[10]

$$\tau_A N^\circ_B = \tau_B N^\circ_A \quad (3)$$

because the predominant equilibrium reaction, such as eq 2, is established for the media containing the BP cation. Hence, it is necessary to investigate the relative importance of chemical exchange dynamics to the observed magnetization recovery curves.

In order to account for the non-single-exponential decays observed in the recovery curves for the compositions located between the two stoichiometries, we assume, for simplicity, the following conditions: (i) If each of two or more overlapping resonances in the ^{27}Al NMR spectra originates from each chloroaluminate i species, each distinct relaxation rate $R_{1,i}$ can occur under the individual time scales. (ii) The Bloch equation holds separately for the recovery of the longitudinal component of magnetization $M_{z,i}$ for each i species. By invoking the master equations for populations, the coupled expressions for the time evolution of the magnetization at sites A and B can be given as follows:[11]

$$d(M_{Z,A} - M^\circ_{Z,A})/d\tau = -(R_{1,A}{}^* + W^\circ_{AB})(M_{Z,A} - M^\circ_{Z,A}) + W^\circ_{BA}(M_{Z,B} - M^\circ_{Z,B}) \quad (4)$$

and

$$d(M_{Z,B} - M^\circ_{Z,B})/d\tau = -(R_{1,B}{}^* + W^\circ_{BA})(M_{Z,B} - M^\circ_{Z,B}) + W^\circ_{AB}(M_{Z,A} - M^\circ_{ZA}) \quad (5)$$

Here, $M_{Z,A}$ and $M_{Z,B}$ are the time-dependent magnetizations in a given site. The constants $M^\circ_{Z,A}$ and $M^\circ_{Z,B}$ indicate the equilibrium values of the magnetization in each site. Furthermore, $R_{1,A}{}^*$ and $R_{1,B}{}^*$ stand for the spin–lattice relaxation rates of each site in the absence of chemical exchange from site A to B. Finally, W°_{AB} (W°_{BA}) is the probability from site A to B (from site B to A) and is defined in eq 3 because W°_{AB} (W°_{BA}) is equal to the inversion of τ_A (τ_B). Under the initial condition $M_{Z,A}$ ($\tau = 0$) $= -M^\circ_{Z,A}$ for the inversion–recovery sequence, the formal solution of the differential equations 3 and 4 is given as

$$M_{Z,\alpha}(\tau) = M^\circ_{Z,\alpha}(1 - 2\exp(-R_{1,\alpha}\tau)) \quad (6)$$

where α stands for A or B; $R_{1,A}$ is expressed in terms of the relaxation parameter $R_{1,A}{}^*$ and the chemical exchange lifetime τ_A (see Appendix). That is, $R_{1,A}$ denotes the spin–lattice relaxation rate of site A in the presence of the chemical exchange, where $R_{1,A}$ is equal to $R_{1,A}{}^*$ when τ_A is infinite, as shown in eq A1–A3. The total longitudinal magnetization M_Z of ^{27}Al in the melt, which consists of the main aluminate species of A and B, has the form

$$M_Z = \sum_{\alpha=A,B} M_{Z,\alpha} \quad (7)$$

A three-parameter nonlinear least-squares analysis of the data for the logarithmic recovery curves vs. τ, which show the non-single-exponential decays (see Figures 2, 4, and 5), yields the relaxation rates $R_{1,A}$ and $R_{1,B}$ and $M^\circ_{Z,A}/(M^\circ_{Z,A} + M^\circ_{Z,B})$. Here, parameters reproduced the experimental points as shown by each dashed line in Figures 2, 4, and 5. The mole fraction X_A of the A sites is determined from the ratio of $M^\circ_{Z,A}/M^\circ_{Z,B}$, in which the correction of the time interval t_d (100 μs to ~300 μs) has been carried out. The assignment of the main ionic and molecular chloroaluminate species in the melt was carried out with the aid of the dependence of the apparent ^{27}Al line width $\Delta\nu_{1/2}$ and the

(8) Hayashi, S.; Hayamizu, K.; Yamamoto, O. *J. Chem. Phys.* **1982**, *76*, 4392.
(9) Ichikawa, K. *J. Chem. Soc., Faraday Trans. 1* **1979**, *75*, 113.
(10) E.g.: Carrington, A.; McLachlan, A. D. "Introduction to Magnetic Resonance"; Harper & Low: New York, 1967; p 204.
(11) Ellis, P. D.; Yang, P. P.; Palmer, A. R. *J. Magn. Reson.* **1983**, *52*, 254.

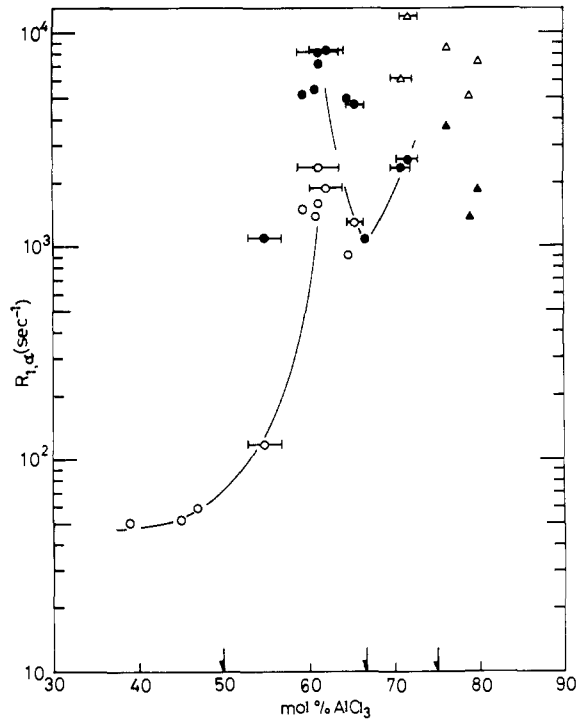

Figure 7. Dependence of the individual spin-lattice relaxation rates $R_{1,\alpha}$ of each chloroaluminate α species on the formal composition at 35 °C. The open and solid marks have been obtained from the nonlinear least-square method: (○) $AlCl_4^-$, (●) $Al_2Cl_7^-$, (△) $Al_3Cl_{10}^-$, and (▲) Al_2Cl_6. The three vertical arrows correspond to the $BPAlCl_4$, $BPAl_2Cl_7$, and $BPAl_3Cl_{10}$ stoichiometric compositions, respectively.

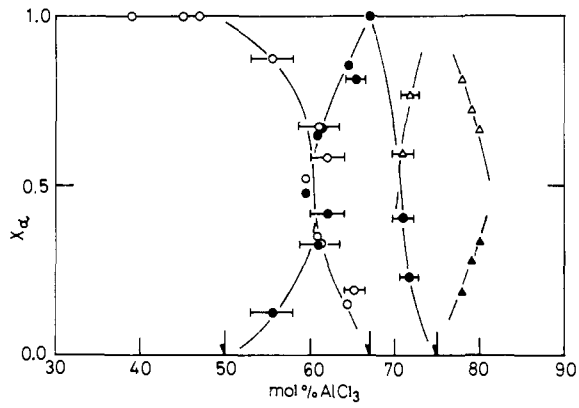

Figure 8. Dependence of the individual mole fractions X_α of each α species on the formal composition. Each mark is defined in Figure 7.

Raman frequency shifts on the formal compositions. Thus, we can summarize as follows: (1) $AlCl_4^-$ and $Al_2Cl_7^-$ exist between 51 and 66 mol % $AlCl_3$, (2) $Al_2Cl_7^-$ and $Al_3Cl_{10}^-$ between 68 and 74 mol % $AlCl_4$, and (3) $Al_3Cl_{10}^-$ and Al_2Cl_6 above 76 mol % $AlCl_3$. Figures 7 and 8 show the appreciable dependence of $R_{1,\alpha}$ and X_α on the main ionic and molecular species, $AlCl_4^-$, $Al_2Cl_7^-$, $Al_3Cl_{10}^-$, and Al_2Cl_6, and on the formal compositions. The magnitude of $R_{1,\alpha}$ is affected by the pair A and B and their concentrations. the chemical exchange from site A to B and vice versa promotes the relaxation of ^{27}Al, because the magnitude of $R_{1,\alpha}$* in the melt, which consists of a main chloroaluminate species (i.e., $R_{1,AlCl_4}$* $\simeq$ 55 s^{-1} at the $AlCl_3$-rich side of 50 mol % $AlCl_3$ and R_{1,Al_2Cl_7}-* $\simeq$ 1000 s^{-1} at the stoichiometry $BPAl_2Cl_7$ or 67 mol % $AlCl_3$), is the minimum of $R_{1,\alpha}$ for all the melts, which show the predominant equilibrium reaction, such as eq 2. Up to 67 mol % $AlCl_3$, the X_α values of the $AlCl_4^-$ and $Al_2Cl_7^-$ species are qualitatively consistent with the potentiometric and Raman spectra investigations. Near the stoichiometric composition (i.e., 67 mol % $AlCl_3$), the chloroaluminate anion is converted virtually to the $Al_2Cl_7^-$ ion. For compositions of less than 53 mol % $AlCl_3$, the FID intensity resulting from the $Al_2Cl_7^-$ ion is almost absent. Above 67 mol % $AlCl_3$, new results on the other $Al_3Cl_{10}^-$ and Al_2Cl_6 species were obtained. A probable peak in the $X(Al_3Cl_{10}^-)$ values locates near the stoichiometry $BPAl_3Cl_{10}$ (or 75 mol % $AlCl_3$): the Al_2Cl_6 species is present in the $AlCl_3$-rich side of 75 mol % $AlCl_3$ as the main species.

At a given set of $R_{1,A}$, $R_{1,B}$, and τ_A/τ_B values calculated from eq 3 and after the assignment of each species, it is necessary to determine the parameters $R_{1,A}$*, $R_{1,B}$*, and τ_A (or τ_B) using each of the equations A1–A3 for sites A and B. In the present study, the magnitude of the exchange lifetime τ_α ranged above 5×10^{-6} s for the main species and was large enough in comparison with the NMR time scale, which was equal to the inversion of the resonance frequency (ca. $5 \cdot 10^{-8}$ s). The chemical exchange rates $W_{AB}°$ (i.e., the inverse of τ_A) are comparable with the relaxation rates, which ranged from 5×10^1 to 2×10^4 s^{-1} (see Figure 7). In the chloroaluminate melts, a remarkably slow exchange took place between the two different species. There exist a number of α species with a larger X_α value which may not take part in the chemical exchange process during $5T_1$, while it takes ca. $5T_1$ for the magnetization to relax until the equilibrium state.

The negative temperature coefficients of the relaxation rates (see Figure 6), which are not affected by the chemical exchange from one species to another, may be equivalent roughly to the dependence of the experimental viscosity η/T on the temperature, because the ^{27}Al nucleus in the complex ions relaxes to the thermal equilibrium through molecular reorientation. We confirmed the agreement between the temperature dependences of η/T of the molten $AlCl_3$ and InI_3 and R_1 of ^{27}Al in molten $AlCl_3$ and ^{115}In in molten InI_3,[12] wherein their melts consist of the dymers Al_2Cl_6 and In_2I_6 as the main species. The temperature dependence of R_1 for the nucleus in the molecular species can be interpreted in terms of the temperature dependence of τ_c or η/T. This is because the correlation time τ_c characterizing the time scale of the fluctuation of the local electric field gradients in nuclear quadrupolar relaxation can be roughly evaluated from

$$\tau_c = \frac{4\pi r_0^3}{3k_B} \frac{\eta}{T} \tag{8}$$

by assuming a rotating spherical molecule with radius r_0.[13] Our conclusions concerning the individual relaxation rates are summarized as follows: (i) R_1*($AlCl_4^-$) $\simeq$ 55 s^{-1} and R_1*($Al_2Cl_7^-$) $\simeq$ 1000 s^{-1} at 35 °C. (ii) The $R_{1,\alpha}$ values increase with increasing the number of ^{27}Al nuclei in each species which has the same charge at the given concentration (i.e., $AlCl_4^-$ < $Al_2Cl_7^-$, $Al_2Cl_7^-$ < $Al_3Cl_{10}^-$, and Al_2Cl_6 < $Al_3Cl_{10}^-$). (iii) The chemical exchange from one species to another promotes the individual relaxations. From the point of view of the available NMR sensitivity, the typical species formation upon successive additions of $AlCl_3$, as well as equilibria i–iii, can by summarized as follows.[14]

$\leq$50 mol % $AlCl_3$ $AlCl_4^-$ ($BPAlCl_4$)

>50 and <67 mol % $AlCl_3$ $2AlCl_4^- = Al_2Cl_7^- + Cl^-$ (i)

=67 mol % $AlCl_3$ $Al_2Cl_7^-$ ($BPAl_2Cl_7$)

>67 and <75 mol % $AlCl_3$ $3Al_2Cl_7^- = 2Al_3Cl_{10}^- + Cl^-$ (ii)

=75 mol % $AlCl_3$ $Al_3Cl_{10}^-$ ($BPAl_3Cl_7$)

>75 and <100 mol % $AlCl_3$ $2Al_3Cl_{10}^- = 3Al_2Cl_6 + 2Cl^-$ (iii)

=pure $AlCl_3$ Al_2Cl_6

Acknowledgment. We are indebted to E. Yamada and Dr. S. Shimokawa (NMR Laboratory, Faculty of Engineering) for the inversion recovery measurements. We thank Professor T. Ishikawa

(12) Ichikawa, K.; Matsumoto, T. *Bull. Chem. Soc. Jpn.* **1982**, 887.
(13) Abragam. A. "The Principles of Nuclear Magnetism"; Oxford University Press: London 1961; p 300.
(14) Øye, H. A., private communication. Our summarization, which was obtained before getting his preprint, on the chloroaluminate species in the molten BPCl + $AlCl_3$ mixtures agrees well with the conclusion that appeared in his preprint.

(Faculty of Engineering) and Dr. J. Sato (Ejima Laboratory, Faculty of Engineering, Tohoku University) for the loan of the crystalline $AlCl_3$. The atomic absorption spectrochemical analysis for Al in the BPCl + $AlCl_3$ mixtures was carried out by the helpful advice of T. Tanaka (Department of Chemistry, Faculty of Science). This work was supported in part by a Grant-in-Aid for Scientic Research No. 58540242 from the Ministry of Education, Science and Culture, Japan.

Appendix

$R_{1,A}$ is the spin-lattice relaxation rate in the presence of chemical exchange from A to B. It is given as follows:

$$R_{1,A} = \frac{D \pm E^{1/2}}{2} \tag{A1}$$

where

$$D = R_{1,A}^* + R_{1,B}^* + \frac{1}{\tau_A} + \frac{1}{\tau_B} \tag{A2}$$

and

$$E = (R_{1,A}^* - R_{1,B}^*)^2 + \frac{4}{\tau_A \tau_B} \tag{A3}$$

Under the condition that the probability for spin transfer from site A to B (or B to A), W°_{AB} (or W°_{BA}), is equal to zero, $R_{1,A}$ is equal to $R_{1,A}^*$. Because of this reason, if $R_{1,A}^*$ is larger than $R_{1,B}^*$, $R_{1,A}$ is given as $(D + E^{1/2})/2$. The other way, if $R_{1,B}^*$ is larger than $R_{1,A}^*$, $R_{1,A}$ is given as $(D - E^{1/2})/2$.

Registry No. Al, 7429-90-5; $AlCl_3$, 7446-70-0; BPCl, 1124-64-7.

Transient Absorption and Two-Step Laser Excitation Fluorescence Studies of the Excited-State Proton Transfer and Relaxation in the Methanol Solution of 7-Hydroxyflavone

Michiya Itoh* and Tomoko Adachi

Contribution from the Faculty of Pharmaceutical Sciences, Kanazawa University, Takara-machi, Kanazawa 920, Japan. *Received December 19, 1983*

Abstract: The methanol solution of 7-hydroxyflavone (7-HF) exhibits dual fluorescence (λ_{max} 410 and 530 nm) with very short lifetimes at room temperature, and the 530-nm fluorescence shows two exponential decays at ~200 K (τ = <0.2 and 0.7 ns). The long-wavelength fluorescence was ascribed to the excited-state tautomer generated by the excited-state proton transfer in the hydrogen bonding complex of 7-HF with two methanol molecules (1:2), which was confirmed by the methanol concentration dependence in tetrahydrofuran of the 530-nm fluorescence intensity. The transient absorption spectra of this solution exhibit two transient absorption bands at 380 and 420 nm with short and long decay times (~400 ns and ~60 μs) in addition to the triplet-triplet absorption band (λ_{max} ~ 370 nm). These transient absorptions were attributable to two ground-state tautomers generated by the excited-state proton transfer and relaxation. The first laser excitation of 7-HF in methanol induces the formation of two unstable ground-state tautomers. The second dye laser excitation of the transient absorption bands delayed from the first one affords two considerably different two-step laser excitation (TSLE) fluorescence spectra (λ_{max} 525-530 and 515-520 nm) of the tautomers. Further, when delay times between the first and second laser pulses were varied (a variable delay technique), the decay times of two ground-state tautomers were determined to be 450 ns and 50-60 μs, which are consistent with those obtained by the transient absorption spectroscopy. These TSLE fluorescence and transient absorption spectra demonstrate that the excited-state proton transfer in the methanol solution of 7-HF may take place, forming two types of phototautomers in the excited state and also in the ground state.

Two-step laser excitation (one or two colors) fluorescence as one of the recent developments of the laser spectroscopy provides us with the reaction kinetics and dynamics of unstable molecules. Recently, a Bell Laboratories group reported the spectra and kinetics of naphthylmethyl radical by means of two-color laser-induced fluorescence experiments.[1] Further, Sitzmann, Wang, and Eisenthal have also determined reaction rate constants of the triplet diphenylcarbene with alcohols by the two-pulse experiment with UV picosecond pulses (one color).[2] At the almost same time, Itoh et al.[3] have reported transient absorption and two-step laser excitation (TSLE, two colors) fluorescence studies of the excited-state and ground-state proton transfer in the methanol solution of 7-hydroxyquinoline (7-HQ).

Numerous investigations of the intra- and intermolecular excited-state proton transfer of the hydrogen bonding systems were reported by nano- and picosecond fluorescence spectroscopy as well as conventional steady-state spectroscopy.[4-11] On the other hand, the transient absorption study that may provide us with valuable information on the proton transfer not only in the excited state but also in the ground state has only been reported in a few papers.[12-14] Recently, Huston et al.[13] have reported that 2-(2-hydroxy-5-methylphenyl)benzotriazole in several solvents shows

(1) Kelly, D. F.; Millton, S. V.; Huppert, D.; Rentzepis, P. M. *J. Phys. Chem.* **1983**, *87*, 1842.
(2) Sitzmann, E. V.; Wang, Y.; Eisenthal, K. B. *J. Phys. Chem.* **1983**, *87*, 2283.
(3) Itoh, M.; Adachi, T.; Tokumura, K. *J. Am. Chem. Soc.* **1983**, *105*, 4828.
(4) Smith, K. K.; Kaufmann, K. J. *J. Phys. Chem.* **1978**, *82*, 2286.
(5) Shizuka, H.; Matsui, S.; Hirata, Y.; Tanaka, I. *J. Phys. Chem.* **1976**, *80*, 2072; **1977**, *81*, 2243 and references therein.
(6) Barbara, P. F.; Brus, L. E.; Rentzepis, P. M. *J. Am. Chem. Soc.* **1980**, *102*, 2786.
(7) Woolfe, G. J.; Thistlethwaite, P. J. *J. Am. Chem. Soc.* **1980**, *102*, 6917 and references therein.
(8) Woolfe, G. J.; Thistlethwaite, P. J. *J. Am. Chem. Soc.* **1981**, *103*, 6916.
(9) Itoh, M.; Tokumura, K.; Tanimoto, Y.; Okada, Y.; Takeuchi, H.; Obi, K.; Tanaka, I. *J. Am. Chem. Soc.* **1982**, *104*, 4146.
(10) Strandjord, A. J. G.; Courtney, S. H.; Friedrich, D. M.; Barbara, P. F. *J. Phys. Chem.* **1983**, *87*, 1125.
(11) Nagaoka, S.; Hirota, N.; Sumitani, M.; Yoshihara, K. *J. Am. Chem. Soc.* **1983**, *105*, 4220.
(12) Hou, S.-Y.; Hetherington, W. M., III; Korenowski, G. M.; Eisenthal, K. B. *Chem. Phys. Lett.* **1979**, *68*, 282.
(13) Huston, A. L.; Scott, G. W.; Gupta, A. J. *J. Chem. Phys.* **1982**, *76*, 4978.
(14) Itoh, M.; Tanimoto, Y.; Tokumura, K. *J. Am. Chem. Soc.* **1983**, *105*, 3339.

0002-7863/84/1506-4320$01.50/0